Methods for Investigating Environmental Noise in Advanced LIGO

Philippe N, Robert S, Anamaria E

Links & Info

- Writing team: Philippe N, Robert S, Anamaria E
- Detchar circulation for comments ~ 1 month, then P&P circulation
- Git repository: https://git.ligo.org/pem/o3-pem-paper
- Issue tracker: https://git.ligo.org/pem/o3-pem-paper/-/issues
- DCC version: https://dcc.ligo.org/P2000343

Section 1: Introduction

- Summary of aLIGO and O1-O3
- How environmental noise impact the interferometers
- Purpose of environmental monitoring:
  - Vetting of gravitational wave events
  - Characterizing and mitigating noise sources
- The paper will describe changes since Effler et al (2015) and discuss aLIGO noise sources and vetting
- Mention non-PEM methods in noise characterization
- Paper outline

Section 2: aLIGO upgrades

Section 2.1: Detector upgrades

- Summary of aLIGO upgrades for that were particularly relevant to PEM

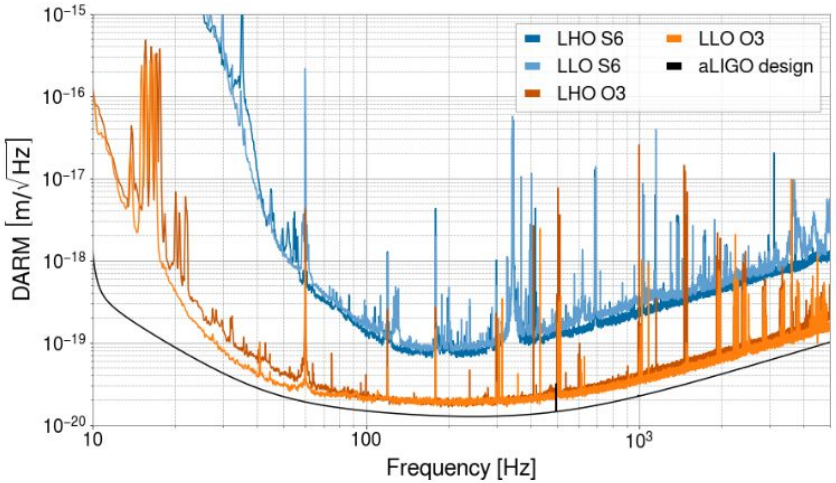

Figure 1: Amplitude spectral densities of the differential arm length displacement (DARM) at the end of S6 (Feb 27 2010 04:27:47 UTC) and during O3 (Mar 20 2020 00:00:00 UTC).

Section 2: aLIGO upgrades

Section 2.2: Environmental monitoring upgrades

- Motivation for various PEM sensor types
- Map of sensors (Fig. 2) and table of PEM sensor models and specs (Tab. 1)
- New/moved accelerometers
- Additional fluxgate magnetometers, e.g. for monitoring lines in electronics racks
- Induction coil magnetometers (LEMIs) for Schumann resonances

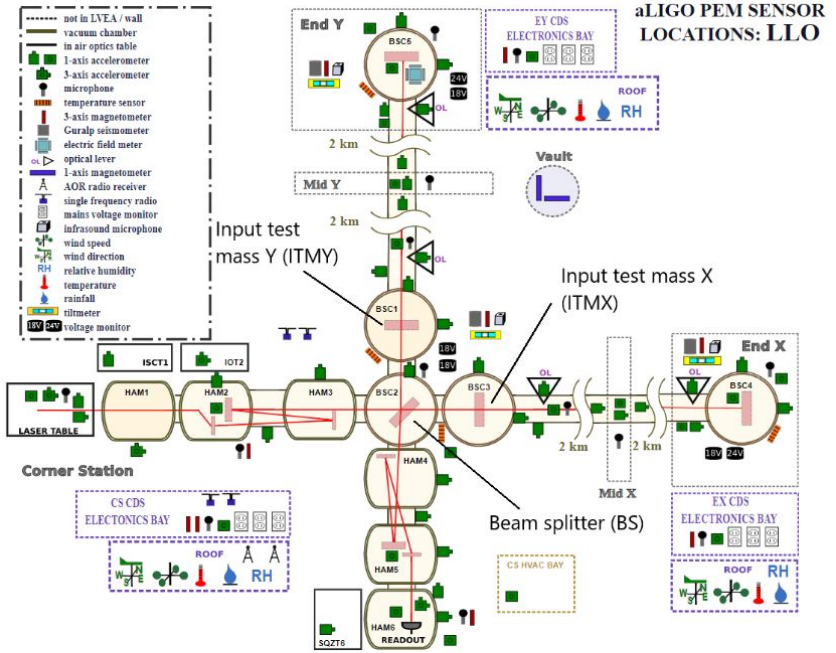

Figure 2: The Physical Environmental Monitoring system layout at the LIGO Livingston detector during O3, as seen on the PEM public website [18]. The path of the main interferometer laser is shown as a red line; core optics, such as the test masses, are represented by rectangles inside the vacuum chambers. The most major changes during aLIGO have been made to the accelerometer locations and the addition of new magnetometers, e.g. in the electronics bays.

Section 3: Coupling functions

- How to compute coupling functions
- Sensor/DARM thresholds for CFs
- Composite CFs

$$\mathrm{CF}(f) = \sqrt{\frac{[Y_{\mathrm{inj}}(f)]^2 - [Y_{\mathrm{bkg}}(f)]^2}{[X_{\mathrm{inj}}(f)]^2 - [X_{\mathrm{bkg}}(f)]^2}}$$

$$\mathrm{CCF}(f_k) = \mathrm{CF}_i(f_k) \text{ where } i = \underset{j \in A}{\mathrm{argmax}} \left(X_j(f_k)\right)$$

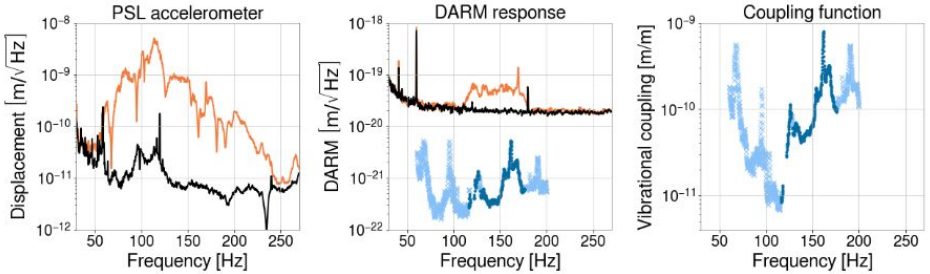

Figure 3: Vibrational coupling excited by a broadband (60-200 Hz) acoustic injection near the output arm of the interferometer. The left plot shows the displacement of an accelerometer in the PSL room during background time (black) and injection time (orange). The middle plot shows the interferometer readout during background time (black) and injection time (orange). Estimated ambient levels for the accelerometer are also shown as dark blue dots, with upper limits shown as light blue crosses; they are produced from the coupling function in the right plot. A vibrational coupling function represents meters of test mass displacement per meter of sensor displacement, hence the units of m/m.

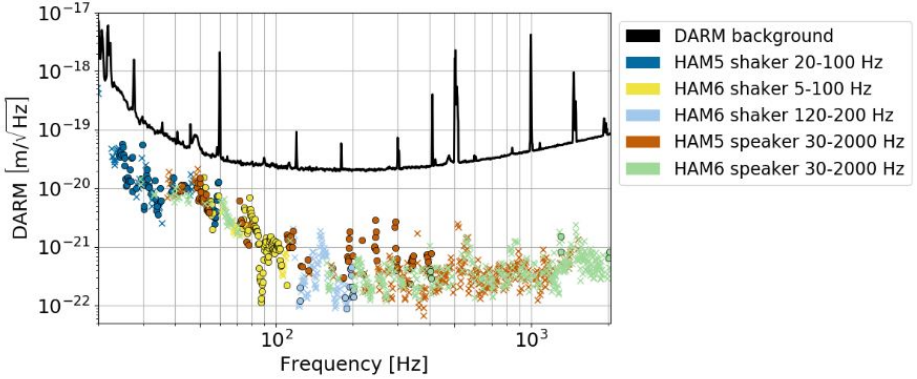

Figure 4: Ambient noise level for the HAM6 Y-axis accelerometer estimated from a composite coupling function, using acoustic and seismic injections near the output arm. For simplicity only five injections were used to produce this example, however in practice the number of injections performed near a sensor can be many times higher.

Section 3: Coupling functions

Section 3.1: Uncertainties and limitations

- We ignore non-linear coupling and up/down-converted noise
- The sensor array is finite, so coupling can vary with injection location (variance is less in sensors close to the coupling site but still usually about a factor of two)
- Sensors can coincide with (anti-)nodes, resulting in spectral artifacts
- We check coupling functions using real-world “injections”, e.g. helicopters, thunder

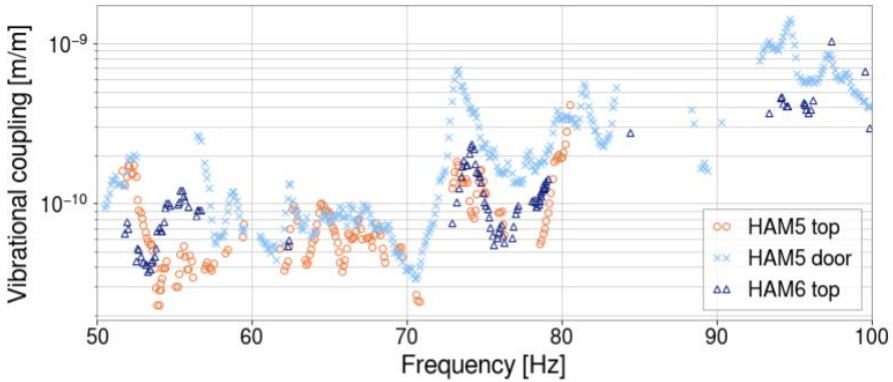

Figure 5: Coupling functions for the HAM5 Y-axis accelerometer from shaking injections made from three different locations (on top of HAM5, on top of HAM6, and on the HAM5 chamber door). Multiple injections at different frequency bands are shown for each source location. On average the coupling measured from different locations varies by to a factor of two.

Section 4: Injection methods

- Discuss general strategy for PEM injections
- Current equipment inventory (Tab. 2)
- Vibrational beat injections
  - Using two shakers at different locations, we inject a line from each, at slightly different frequencies (e.g. 100 Hz and 100.01 Hz if studying coupling at 100 Hz) to produce beats
  - Use spectrograms over many beat periods to see what sensors line up best with DARM

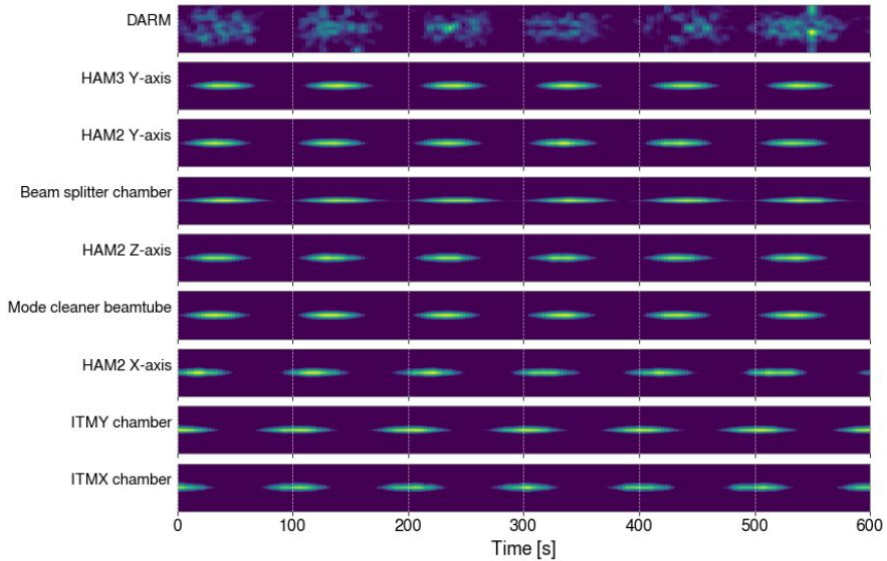

Figure 6: Spectrograms of a beat injection using two shakers to localize the coupling site responsible for a 48 Hz peak in the DARM spectrum. The beat envelope in DARM best matches the timing of the beat envelope in the HAM3 chamber door accelerometer, suggesting that the dominant coupling site causing the 48 Hz peak is near or on the HAM3 chamber door.

Section 4: Injection methods

- Impulse injections
  - Use time series and spectrograms to analyze propagation delays, coupling, and frequency structure of impulses
- New wall-mounted coils for weekly magnetic injections/analysis

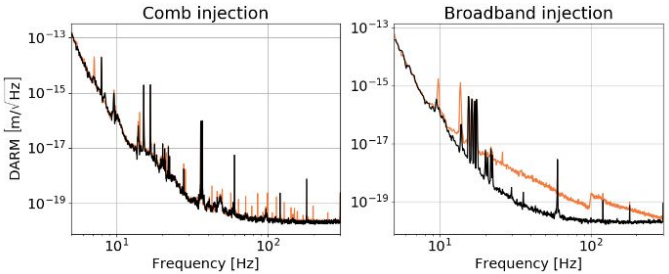

Figure 8: DARM response to old (left, comb) and new (right, broadband) magnetic injections. Black and orange lines show the DARM ASD before and during the injections, respectively. The comb injection curve is a composite of multiple comb injections, with fundamental frequencies of 7.1 Hz, 14.2 Hz, and 49.7 Hz, made at different times. The broadband injection spectrum is a composite of a 10-100 Hz injection and a 100-1000 Hz injection made at different times.

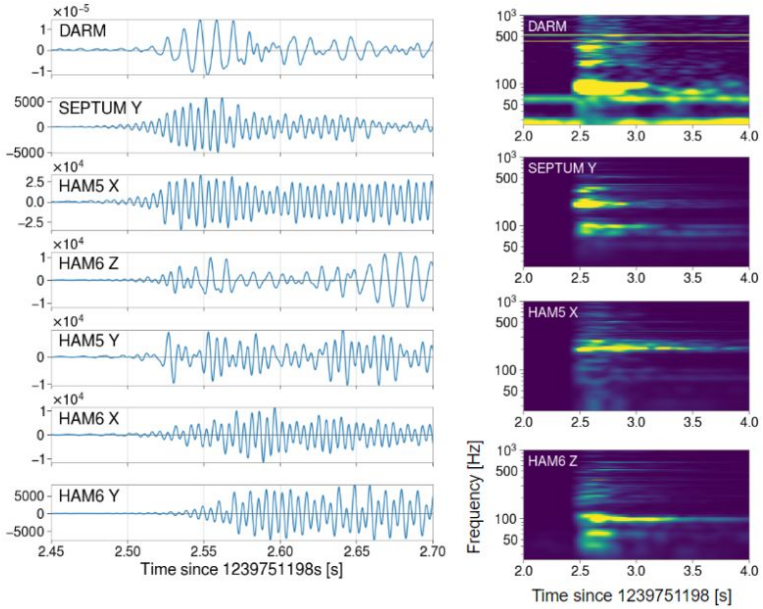

Figure 7: Left: Time series of an impulse injection signal in DARM and various output optics accelerometers. Multiple sensors observe a time-of-arrival matching that of DARM, but the septum accelerometer is the most consistent between different injections (although only one injection is shown here for brevity). Right: Spectrograms of the same impulse injection for DARM and the three sensors with the closest matching time-of-arrival to DARM. The matching frequency structure of the septum accelerometer to DARM further supports the septum (separating the HAM5 and HAM6 chambers) as a dominate coupling site in the output arm.

Section 5: Mitigation of environmental effects in Advanced LIGO

Section 5.1: Seismic and acoustic influences

- Input beam jitter
- Vibrational coupling at resonances of the vibration isolation system
- Coupling of wind through ground tilting in the 0.1 Hz band
- Vibration modulation of scattered light paths

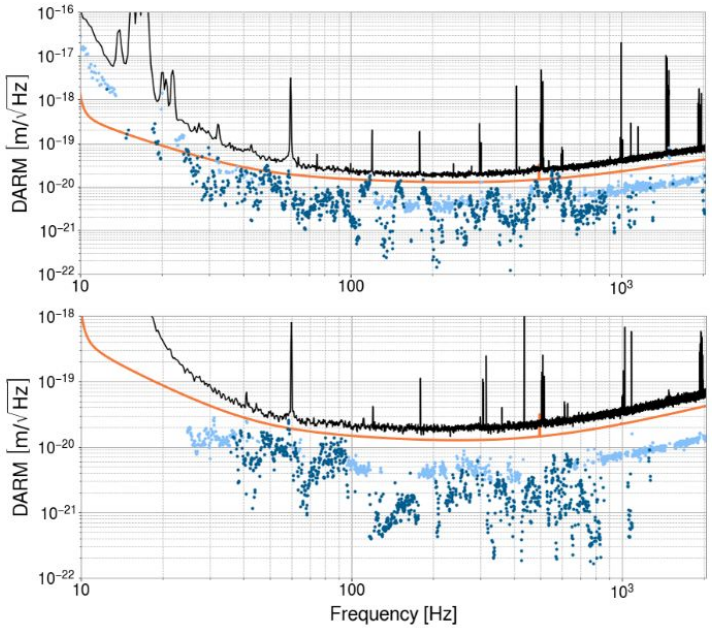

Figure 9: Ambient vibrational noise at LHO (top) and LLO (bottom), shown in dark blue (measurements) and light blue (upper limits). The black and orange lines show the DARM background and the aLIGO design sensitivity.

Section 5: Mitigation of environmental effects in Advanced LIGO

Section 5.2: Magnetic influences

- Coupling from permanent magnets in suspensions still close to design sensitivity at low frequency
- Magnetic coupling above 30 Hz now dominated by cables/connectors

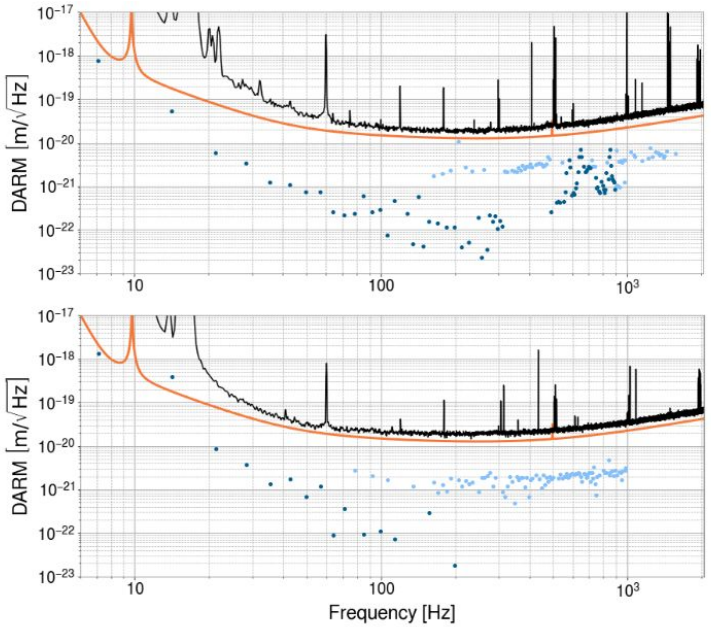

Figure 10: Ambient magnetic noise at LHO (top) and LLO (bottom), shown in dark blue (measurements) and light blue (upper limits). The black and orange lines show the DARM background and the aLIGO design sensitivity. Points are shown for multiples of 7.1 Hz because most of the injections performed were 7.1 Hz comb injections. Data from broadband injections is included, but only at the comb frequencies due to only having one broadband injection source at the time.

Section 5: Mitigation of environmental effects in Advanced LIGO

Section 5.3: Other influences

- Dust and particulates causing glitches in DARM
- Low-frequency noise from HVAC air and cooling water flow
- Moved temperature sensors from walls to vacuum chambers
- Temperature control on electronics
- Other site activities (vehicles, motor-driven equipment)
- Humidity affecting blip glitches in O1/O2

Section 6: Event validation

- Environmental noise can be correlated b/w sites, something that sets it apart from other types of detector noise
- Summary of GW150914 and GW170817 environmental noise vetting
- Estimating DARM contributions of environmental transients now mostly automated w/ DQR
- Human input still used, especially for exceptional event candidates

Section 7: Conclusion

- Summary of paper
- Mention future work, preparations for O4

Links & Info

- Writing team: Philippe N, Robert S, Anamaria E
- Detchar circulation for comments ~ 1 month, then P&P circulation
- Git repository: https://git.ligo.org/pem/o3-pem-paper
- Issue tracker: https://git.ligo.org/detchar/o3-detchar-paper/-/issues/1
- DCC version: https://dcc.ligo.org/P2000343